

Article

Quantum Work from a Pseudo-Hermitian Hamiltonian

Marta Reboiro^{1,2,*}  and Diego Tielas^{1,2,3,†} ¹ Institute of Physics of La Plata (IFLP), Boulevard 113 & 63, La Plata C.P. 1900, Argentina² Department of Physics, University of La Plata, C.C. 67, La Plata C.P. 1900, Argentina³ Faculty of Engineering, National University of La Plata, Av. 1 750, La Plata C.P. 1900, Argentina

* Correspondence: reboiro@fisica.unlp.edu.ar; Tel.: +54-0221-644-3202

† These authors contributed equally to this work.

Abstract: In this work, we study the thermodynamics of a hybrid system based on the Da Providencia–Schütte Hamiltonian. The model consists of bosons, i.e., photons in a cavity, interacting with an ensemble of spins through a pseudo-Hermitian Hamiltonian. We compute the exact partition function of the system, and from it, we derive the statistical properties of the system. Finally, we evaluate the work that can be extracted from the system by performing an Otto cycle and discuss the advantages of the proposed pseudo-Hermitian interaction.

Keywords: non-Hermitian dynamics; pseudo-hermicity; quantum work; Da Providencia–Schütte model

1. Introduction

Quantum thermodynamics [1,2] has emerged as a promising research field both from an experimental [3–6] and from a theoretical perspective [7–14]. Statistical fluctuations in single quantum systems satisfy new laws known as quantum fluctuation theorems. Some of the fundamental questions have been addressed by Jarzynski and co-workers [7–10]. In [7], an expression for the equilibrium free energy difference between two configurations of a system, in terms of the work performed in parametrically switching from one configuration to the other, is given. The work reported in [8] settles the statements of the second law of thermodynamics through a generalization of the ones of Kelvin–Planck, Clausius, and Carnot. The authors of [9] discuss the statistics of heat exchange between two classical or quantum finite systems initially prepared at different temperatures. Many questions, such as the role of entanglement and coherence, still remain open [15–19]. The answer to these questions may lead to the development of quantum heat engines and refrigerators, as well as simple descriptions of quantum many-body systems. Recently, the authors of [11] present the First and Second Laws of Quantum Thermodynamics from a Microscopic Definition of Entropy. In the same direction, the work presented in [12] addresses the emergence of thermodynamic laws from quantum mechanics, from a viewpoint based on the connection of quantum thermodynamics with the theory of open quantum systems. In [13], the analysis of thermodynamic uncertainty principles has been conducted. The authors of [17] have shown that the energetic contribution of the dynamics of coherence is an essential topic to address for the consistency of the theory of quantum thermodynamics. An increasing number of works are devoted to the design of quantum heat engines and refrigerators. Among others, we can mention the heat machines whose working substance performs an Otto cycle. Some examples have been presented in [16,17,20–23]. In [20], a quantum Otto engine using two-interacting spins as its working medium is analyzed within the framework of stochastic thermodynamics. The authors of [21] analyze the efficiency of the quantum Otto cycle applied to a superconducting cavity. In [22], the statistic work of a Fermi gas when a localized scattering potential is suddenly introduced in a Fermi sea is analyzed. The authors of [23] investigate the particle–number dependence of some features of the out-of-equilibrium dynamics of d-dimensional Fermi gases in the dilute



Citation: Reboiro, M.; Tielas, D.

Quantum Work from a Pseudo-Hermitian Hamiltonian.

Quantum Rep. **2022**, *4*, 589–603.

[https://doi.org/10.3390/](https://doi.org/10.3390/quantum4040043)

[quantum4040043](https://doi.org/10.3390/quantum4040043)

Academic Editor: J. Gonzalo Muga

Received: 1 November 2022

Accepted: 9 December 2022

Published: 13 December 2022

Publisher's Note: MDPI stays neutral with regard to jurisdictional claims in published maps and institutional affiliations.



Copyright: © 2022 by the authors. Licensee MDPI, Basel, Switzerland. This article is an open access article distributed under the terms and conditions of the Creative Commons Attribution (CC BY) license (<https://creativecommons.org/licenses/by/4.0/>).

regime. In [16], heat engines whose working substance are made of two coupled qubits performing a generalized Otto cycle have been studied in connection with the properties of coherence and entanglement.

Since the pioneering work of Bender [24,25] on Hamiltonians which obey Parity-Time Reversal (PT)-symmetry, many works have been written, setting the basis of the dynamics of non-Hermitian systems. The Hamiltonians which are invariant under PT-symmetry belong to the class of pseudo-Hermitian Hamiltonians [26,27]. A Pseudo-Hermitian operator is an operator which is similar to its adjoint. The spectrum of pseudo-Hermitian Hamiltonians may contain complex conjugate pairs. In terms of the space of parameters of the model, two dynamical phases can be distinguished. In one of the regions, the spectrum is real (symmetry phase), and, in the other complex conjugate, pairs appear (phase with broken symmetry). The border between both regions consists of Exceptional Points (EPs). At these points, two or more eigenvalues and their corresponding eigenstates are coalescent. Concerning the thermodynamics of this class of Hamiltonians, it has been proved that the quantum Jarzynski equality [7] can be generalized to PT-symmetric quantum mechanics with an unbroken phase [28]. The concept was extended to pseudo-Hermitian in the symmetry phase in [29]. In a recent paper [30], some aspects of quantum thermodynamics under the background of non-Hermitian quantum mechanics have been analyzed in connection to a quantum harmonic oscillator.

In this work, we proposed to study the amount of work we can extract from an Otto cycle when the working substance is a hybrid system composed of bosons and spins. The system interacts through a Hamiltonian based on a generalization of Da Providencia-Schütte Hamiltonian [31]. We have included an asymmetry parameter in the interaction to account for the impurities that can be present in the system [32–34]. Thus, the interaction is constructed as pseudo Hermitian. The study is focused on the influence of the asymmetry parameter on the extracted work.

The work is organized as follows: In Section 2, we describe the model and the methods we have employed. We review the fundamentals of pseudo-Hermiticity and its application to our model. In Section 3, we analyze the statistical properties of the system and the efficiency of the Otto cycle, both as a heat machine and as a refrigerator. Conclusions are drawn in Section 4.

2. Materials and Methods

The model of Da Providencia and Shütte [31] has been intensively studied in different physical contexts. In particular, it is adequate to describe systems that exhibit condensate phases [35–38]. In a recent experiment, [39], the generation of pairs of photons in a cavity and electrons has been reported. The Hamiltonian model [31] can be written as

$$H_{DP} = \frac{1}{2}\omega_f S_0 + \omega_b b^\dagger b + g(S_+ b^\dagger + S_- b), \quad (1)$$

where b and b^\dagger are the annihilation and the creation boson operators associated with a harmonic oscillator of energy ω_b , respectively. The operators $\{S_+, S_-, S_0\}$ obey a $su(2)$ algebra, and they are used to model a two-level system of N_S spins, ω_f being the separation in the energy of the levels. The coupling constant is denoted by g .

The Hamiltonian H_{DP} is invariant with respect to the operator $\hat{\mathcal{L}} = b^\dagger b - S_0$. The model exhibits two different phases. In the normal phase, the minimum value of energy is an eigenstate of $\hat{\mathcal{L}}$ with eigenvalue zero, while, in the deformed phase, the ground state corresponds to an eigenstate of $\hat{\mathcal{L}}$ with eigenvalue non-zero that is a condensate. When the ground state corresponds to an eigenstate of $\hat{\mathcal{L}}$ with positive eigenvalue L , the ground state is a boson condensate, while, with $L < 0$, we have a condensate of spins [31].

The boson–fermion representation of the model and its behavior at finite temperature have been discussed in [40,41]. In this work, we shall analyze the properties of a modified pseudo-Hermitian Hamiltonian

$$H = \frac{1}{2}\omega_f S_0^2 + \omega_b b^\dagger b + g(S_+ b^\dagger + \alpha S_- b), \tag{2}$$

where α is a real parameter which we have introduced as an asymmetry in the interaction between the spins and the bosons. It accounts for the impurities of the system. Similar proposals can be found in [32–34]. The proposed Hamiltonian preserves the invariance under $\hat{\mathcal{L}}$.

As a consequence of the pseudo-Hermiticity of the Hamiltonian H , it exists an operator τ positive defined such that $H^\dagger \tau = \tau^{-1} H$. The operator τ serves as a metric operator, and we can define a vector space Φ with a new inner product $\langle \cdot | \cdot \rangle_\tau$.

Let us denote by $\{|\tilde{\phi}_n\rangle\}$ the set of eigenstates of H , $H|\tilde{\phi}_n\rangle = \tilde{E}_n|\tilde{\phi}_n\rangle$, and $\{|\bar{\psi}_m\rangle\}$ those of H^\dagger , $H^\dagger|\bar{\psi}_m\rangle = \bar{E}_m|\bar{\psi}_m\rangle$. It can be shown that $\{|\tilde{\phi}_n\rangle, |\bar{\psi}_m\rangle\}$ forms a complete bi-orthogonal set

$$\langle \bar{\psi}_m | \tilde{\phi}_n \rangle = \delta_{nm}, \quad \bar{E}_n = \tilde{E}_n^*. \tag{3}$$

The operator τ can be constructed as

$$\tau = \sum_m |\bar{\psi}_m\rangle\langle\bar{\psi}_m|, \quad \tau^{-1} = \sum_m |\tilde{\phi}_m\rangle\langle\tilde{\phi}_m|, \tag{4}$$

so that $|\bar{\psi}_n\rangle = \tau|\tilde{\phi}_n\rangle$, and $|\tilde{\phi}_n\rangle = \tau^{-1}|\bar{\psi}_n\rangle$, being

$$\mathbb{1} = \sum_v |\tilde{\phi}_v\rangle\langle\bar{\psi}_v|. \tag{5}$$

The new inner product is given by

$$\langle \cdot | \cdot \rangle_\tau : \Phi \times \Phi \rightarrow \mathbb{C}, \quad \langle \tilde{\phi}_v | \tilde{\phi}_{v'} \rangle_U = \langle \tilde{\phi}_v | U | \tilde{\phi}_{v'} \rangle. \tag{6}$$

Another characteristic of the pseudo-Hermiticity of the Hamiltonian H of Equation (2) is that the corresponding spectrum is formed either by real or by complex conjugate pairs of eigenvalues. In the model parameter space, the real spectrum corresponds to the symmetry phase while the complex pair conjugate spectrum corresponds to the phase of broken symmetry. The limiting points of these two dynamical phases are called Exceptional Points (EPs). At these points, two or more eigenvalues and their corresponding eigenstates are coalescent. For the Hamiltonian of Equation (2), the EP takes place for $\alpha < 0$. From the mathematical point of view, for $\alpha > 0$, the spectrum of H is real and, for some value of $\alpha < 0$, complex pair conjugate eigenvalues are present.

The grand partition function at a temperature T can be obtained from the density matrix $\rho = e^{-\beta(H-\mu N)}$, with $\beta = (k_B T)^{-1}$ and μ being the chemical potential as

$$\mathcal{Z} = \text{Tr}\rho = \sum_n \langle \tilde{\phi}_n | \rho | \tilde{\phi}_n \rangle_\tau = \sum_n \langle \tilde{\phi}_n | \tau \rho | \tilde{\phi}_n \rangle = \sum_n \langle \bar{\psi}_n | \rho | \bar{\psi}_n \rangle_\tau. \tag{7}$$

It has been proved in [29] that, when the eigenvalues of the Hamiltonian appear as complex conjugate pairs, \mathcal{Z} takes real values.

From \mathcal{Z} , we can derive the thermodynamics of the system, i.e., we can compute the entropy, S , the free energy, F , the internal energy, U , and the specific heat, C , as usual:

$$\begin{aligned} F &= -\frac{1}{\beta} \ln(\mathcal{Z}) + \mu \langle N \rangle, & U &= -\frac{\partial \ln \mathcal{Z}}{\partial \beta} + \mu \langle N \rangle, \\ S &= -\frac{\partial F}{\partial T} \Big|_{V, \mu}, & C &= \frac{\partial U}{\partial T} \Big|_{V, \mu}, \end{aligned} \tag{8}$$

We fix μ by imposing that $\langle N \rangle$ be equal to the number of spins, N_S , of the system.

Let us briefly review the derivation of the exact grand partition function for the Hamiltonian of Equation (2). For further details, the reader is kindly referred to [41].

We assume that the model space for the spins consists of two levels, each with degeneration 2Ω . Thus, in the grand canonical ensemble, the number of spins, N_S , varies from 0 to 4Ω . The normalized state of l -bosons shall be denoted by $|l\rangle$.

We shall give the basis of the physical space in terms of the set the vectors

$$\{|\epsilon_1 k_1, \epsilon_2 k_2, \dots, \epsilon_n k_n\rangle \otimes |l\rangle\}, \tag{9}$$

ϵ_i is the index corresponding to levels, k represents substates, and i reads for the partition with i particles and n is the particle number of the configuration. Thus, $\epsilon_i \in \{1, 2\}$, $k_i \in \{1, \dots, 2\Omega + 1\}$, $i \in \{1, 2, \dots, n\}$, $n \in \{1, 2, \dots, 4\Omega\}$ and $l \in \{0, \dots, \infty\}$. The dimension of the spin subspace $2^{4\Omega}$, while the bosonic subspace has an infinite dimension.

We aimed to decompose the spin subspace into invariant and irreducible subspaces. The distribution of a given number of particles on two degenerate levels can be represented by numbers ν_1 and ν_2 , i.e., ν_1 is the number of sublevels which are occupied by particles in both the lower and the upper levels, ν_2 is the number of sublevels which are unoccupied in the lower and upper levels. The distribution of the particles on the 2τ sublevels determines the quasispin S of the state, with $2\tau = 2\Omega - \nu_1 - \nu_2$. The number of particles in this configuration is $n = 2(\tau + \nu_1)$. We shall call $\Gamma_{k_1, k_2, \dots, k_{2(\tau+\nu_1)}}$ the subspace of states with ν_1 occupied- and ν_2 unoccupied-sublevels. The dimension is $2^{2\tau}$. They are $(2\Omega)! / ((2\tau)! \nu_1! \nu_2!)$ different subspaces $\Gamma_{k_1, k_2, \dots, k_{2(\tau+\nu_1)}}$. Each of these subspaces can be decomposed into irreducible ones with multiplicities

$$g_k^\tau = \frac{(2\tau)!}{k!(2\tau - k)!} - \frac{(2\tau)!}{(k - 1)!(2\tau - k + 1)!}.$$

The exact grand partition function can be written

$$\mathcal{Z}(\beta) = \sum_{\tau \nu_1 \nu_2} \frac{2\Omega!}{(2\tau)! \nu_1! \nu_2!} \sum_k g_k^\tau \sum_{L, m} \exp\left[-\beta(E_{L, m}^{\tau-k} - 2\mu(\tau + \nu_1))\right]. \tag{10}$$

In writing $\mathcal{Z}(\beta)$, we have used the fact that the Hamiltonian of Equation (2) commutes with the operator $\hat{\mathcal{L}}$. Thus, its eigenvalues can be given in terms of the eigenvalue L of $\hat{\mathcal{L}}$.

3. Results and Discussion

In this section, we shall present results for a system modeled by the Hamiltonian of Equation (2).

As reported in [31], for $\alpha = 1$, the spectrum depends on the values of the dimensionless constant $x_{DP} = g\sqrt{\Omega}/(\omega_f \omega_b)$. For values of $x_{DP} \leq 1$, the ground state is an eigenstate of $\hat{\mathcal{L}}$ with eigenvalue $L = 0$, while for values of $x_{DP} > 1$ the minimum value of the energy of the spectrum of H_{DP} corresponds to a state with $L \neq 0$. The corresponding dimensionless constant for the pseudo-Hermitian Hamiltonian H of Equation (2) can be set as $x = g\sqrt{\Omega \alpha}/(\omega_f \omega_b)$. The same trend is true for the pseudo Hermitian Hamiltonian H of Equation (2) in terms of x . That is, the minimum value of the energy in the normal phase ($x < 1$) is achieved at the value $L = 0$, while in the deformed phase $L \neq 0$. For $\alpha < 0$, complex pair conjugate eigenvalues are present in the spectrum, and EPs occur for values $\alpha < 0$.

For simplicity, we shall take the Boltzmann constant as $k_B = 1$, and we shall measure the energy in units of $\sqrt{\omega_f \omega_b}$. We shall fix the number of spins to $N_S = 4$, $\Omega = 2$, and $\omega_f = \omega_b = 1$.

As pointed out before, for values of $\alpha < 0$, EPs are present. As an example, in Figure 1, we plot the eigenvalues of H of Equation (2) as a function of α for $x = 1$ for two different values of L .

In Figures 2 and 3, we show the behavior of the entropy and the internal energy, respectively. The curves correspond to different values of the dimensionless coupling constant x . In Figure 2, from left to right, the values of x take the values 0.5, 1, 1.5, 2, 2.5, 3, respectively. The same for Figure 3, but from the up to the down curve. Panels (a), (b), (c), and (d), stand for values of the asymmetry parameter $\alpha = 1, 1.5, 0.5$ and 0.1 , respectively. The curves of both entropy and internal energy are continuous as a function of the temperature but displayed a pronounced change in the slope at low temperatures, this is the signature of a second-order phase transition as a function of the temperature. This transition occurs to greater values of T as α increases.

In Figures 4 and 5, we have displayed the behavior of the temperature and the internal energy, as a function of the dimensionless parameter x , at constant values of the entropy. The entropy S takes the values 2 to 8, in steps of one, in increasing order from the down curve to the up curve. As in the previous figures, panels (a), (b), (c), and (d), stand for values of the asymmetry parameter $\alpha = 1, 1.5, 0.5$, and 0.1 , respectively. As can be inferred from Figure 4, the temperature remains almost constant along the adiabatic up to values of $x = 1$. The same is true for the internal energy displayed in Figure 5. As α tends to zero, both temperature and entropy remain constant along the adiabatic.

In Figures 6 and 7, we show the behavior of the entropy and the internal energy, respectively. The curves correspond to different values of the dimensionless coupling constant x . In Figures 6 and 7, from the up to the down curve, the values of x take the values 0.5, 1, 1.5, and 2, respectively. Panels (a), (b), (c), and (d) stand for values of the asymmetry parameter $\alpha = -1.25, -1.0, -0.75$, and -0.362 , respectively. As seen in Figure 1, at the value $\alpha = -0.362$, the system shows a EP for $x = 1$. Though the partition function is real [8,29], the behavior of entropy and the internal energy, for large values of x , may show anomalies at low temperatures. This is because we are working with an effective interaction that takes into account the effect of the environment, and not with the whole system [42–44].

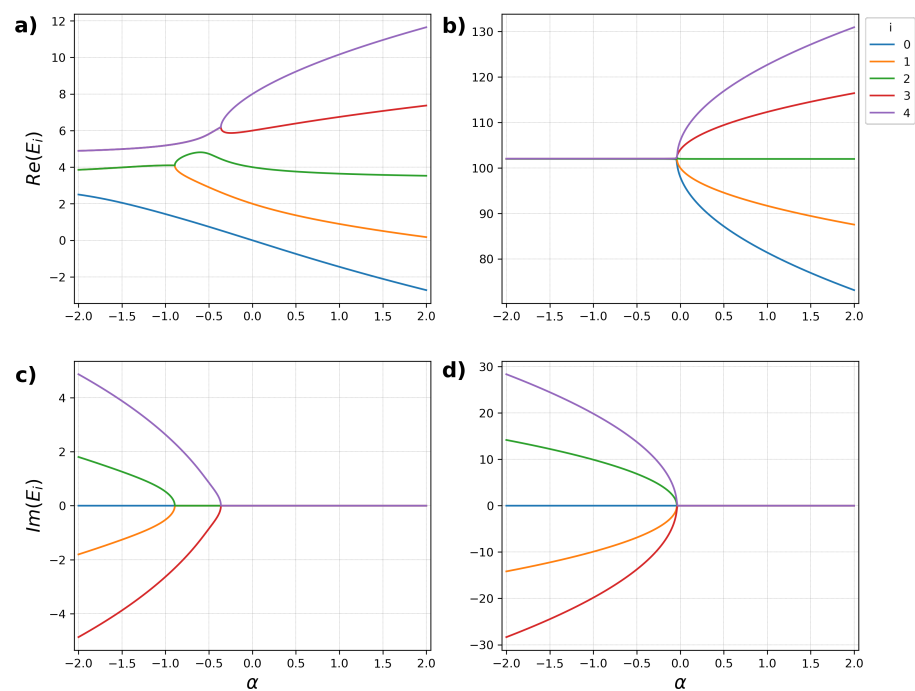


Figure 1. The behavior of the eigenvalues of H of Equation (2) are displayed as a function of α . The diagonalization was performed for a system with $N_s = 4$, $\Omega = 2$ and $x = 1$. Panels (a,b) correspond to values of $L = 2$, and (c,d) to values of $L = 100$. We plot the real part of the eigenvalues in (a,c), and the imaginary part in (b,d).

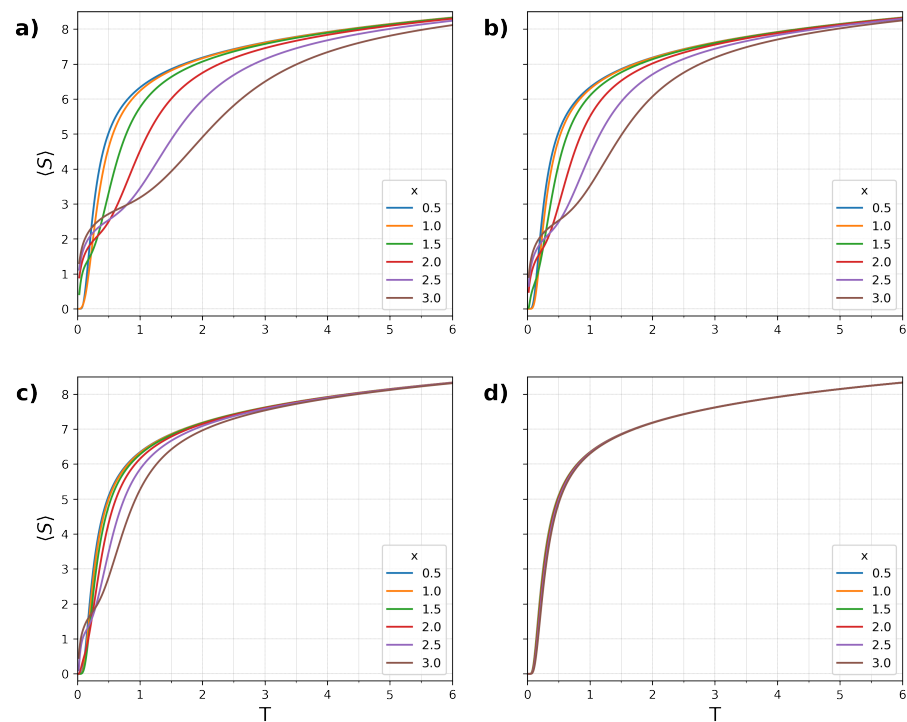


Figure 2. The behavior of the entropy is displayed as a function of the temperature. The curves correspond to different values of the a -dimensional coupling constant x . From left to right, the values of x take the values 0.5, 1, 1.5, 2, 2.5, and 3, respectively. (a–d) stand for values of the asymmetry parameter $\alpha = 1, 1.5, 0.5,$ and $0.1,$ respectively.

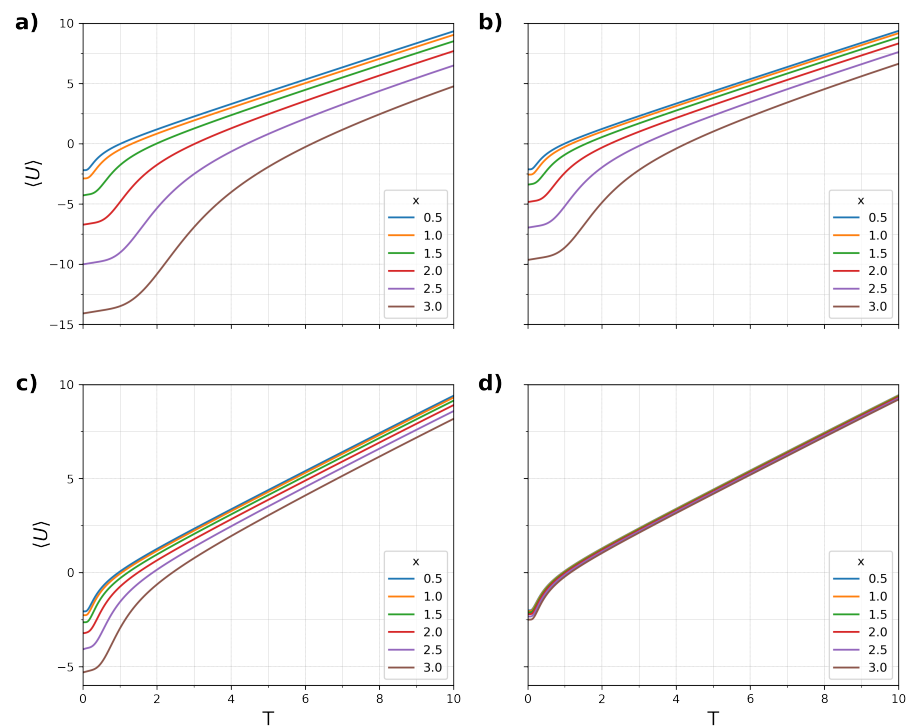


Figure 3. The results that we have obtained for the internal energy as a function of the temperature are presented in this figure. The curves correspond to different values of the dimensionless coupling constant x , from the up to the down curve x takes the values 0.5, 1, 1.5, 2, 2.5, 3 respectively. (a–d) stand for values of the asymmetry parameter $\alpha = 1, 1.5, 0.5,$ and $0.1,$ respectively.

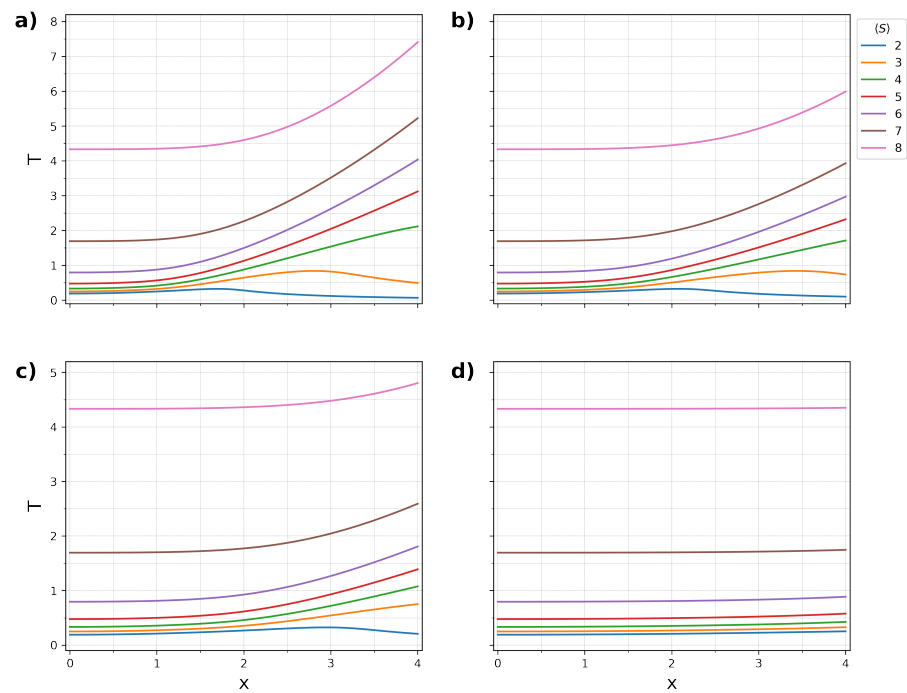


Figure 4. This figure shows the behavior of the temperature, as a function of the dimensionless parameter x , at constant values of the entropy. The entropy S takes the values 2 to 8, in steps of one, in increasing order from the down curve to the up curve. As in the previous figures, (a–d) stand for values of the asymmetry parameter $\alpha = 1, 1.5, 0.5$, and 0.1 , respectively.

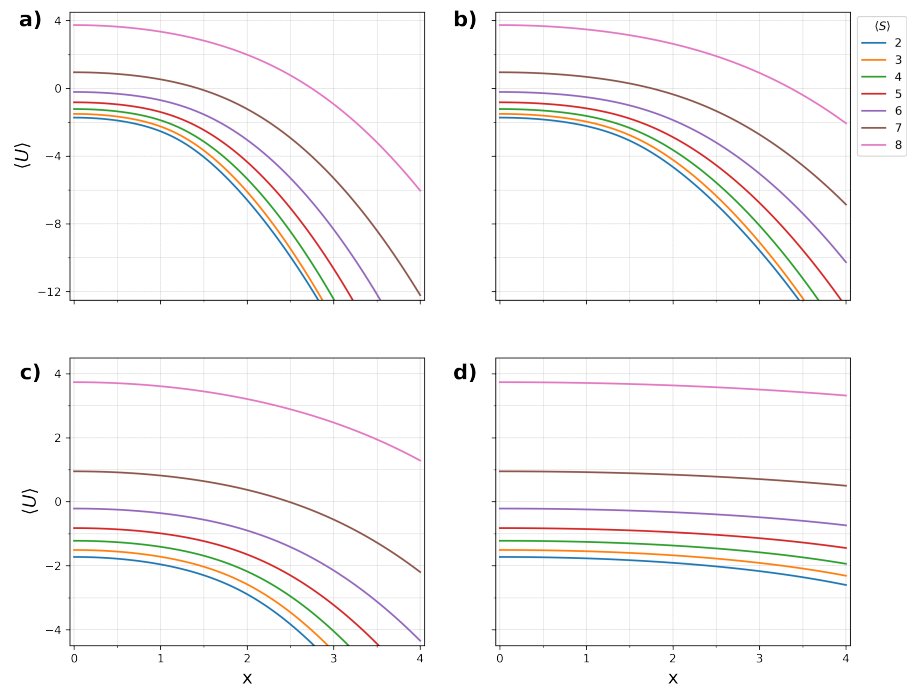


Figure 5. The behavior of the internal energy as a function of the dimensionless parameter x , at constant values of the entropy, is presented. The entropy S takes the values 2 to 8, in steps of one, in increasing order from the down curve to the up curve. As in the previous figures, (a–d) stand for values of the asymmetry parameter $\alpha = 1, 1.5, 0.5$ and 0.1 , respectively.

The different thermodynamical quantities are depicted for negative values of the asymmetry parameter α in Figures 6–13.

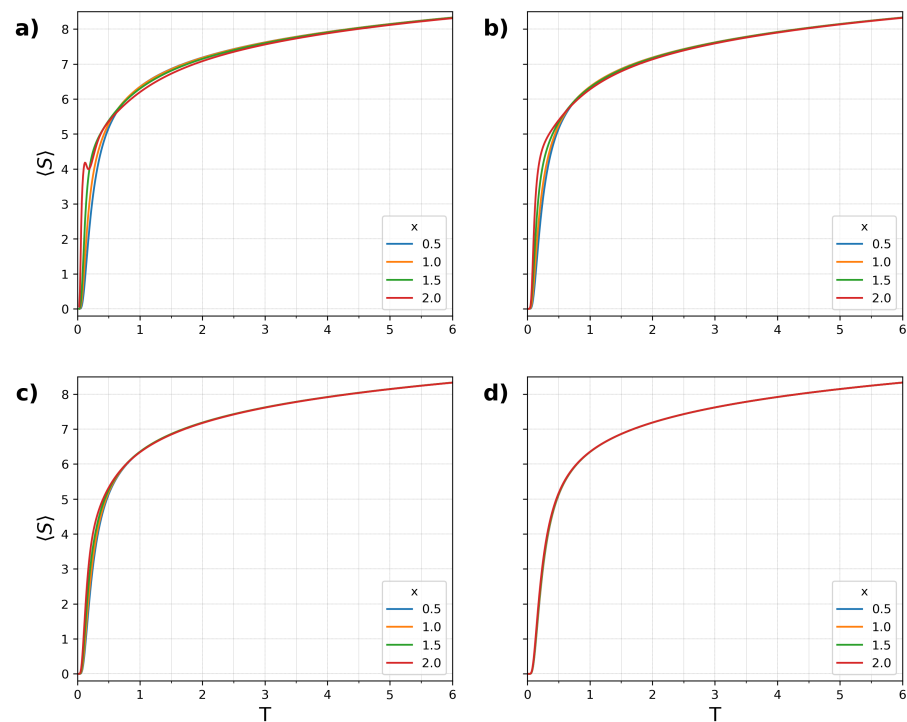


Figure 6. The behavior of the entropy is displayed as a function of the temperature. The curves correspond to different values of the dimensionless coupling constant x . From left to right, the values of x take the values 0.5, 1, 1.5, and 2, respectively. (a–d) stand for values of the asymmetry parameter $\alpha = -1.25, -1.0, -0.75,$ and $-0.362,$ respectively.

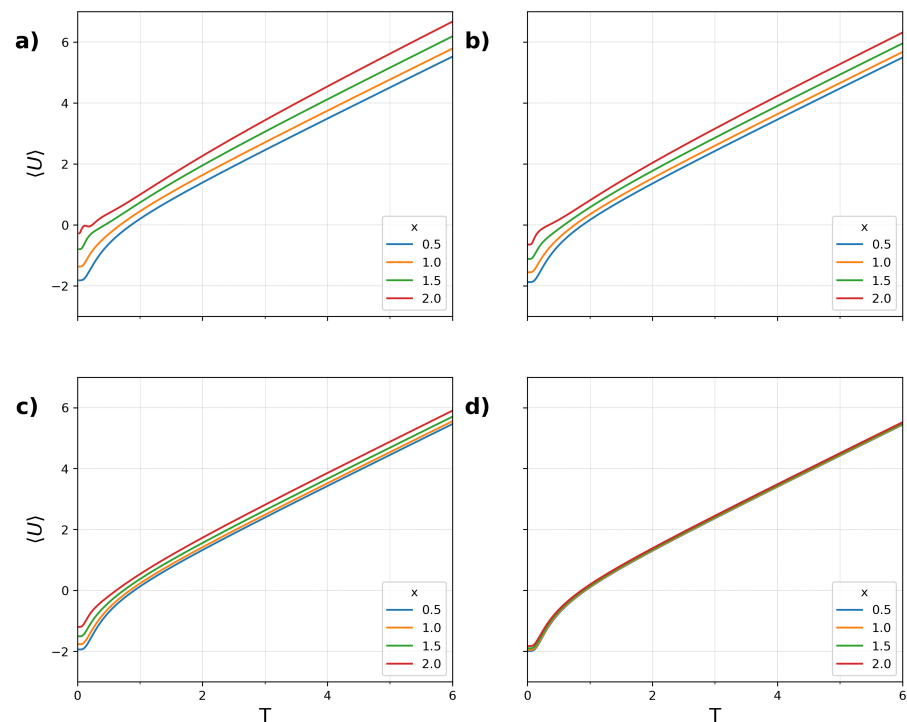


Figure 7. The results that we have obtained for the internal energy as a function of the temperature are presented in this Figure. The curves correspond to different values of the dimensionless coupling constant x , from the up to the down curve x takes the values 0.5, 1, 1.5, and 2, respectively. (a–d), stand for values of the asymmetry parameter $\alpha = -1.25, -1.0, -0.75,$ and $-0.362,$ respectively.

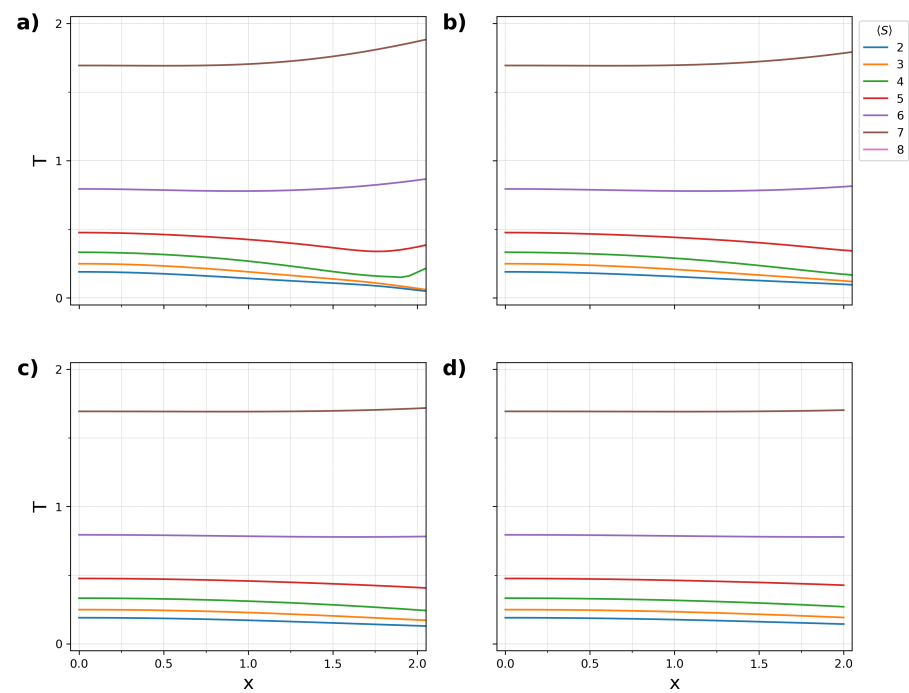


Figure 8. This figure shows the behavior of the temperature, as a function of the dimensionless parameter x , at constant values of the entropy. The entropy S takes the values 2 to 8, in steps of one, in increasing order from the down curve to the up curve. As in the previous figures, (a–d) stand for values of the asymmetry parameter $\alpha = -1.25, -1.0, -0.75,$ and -0.362 , respectively.

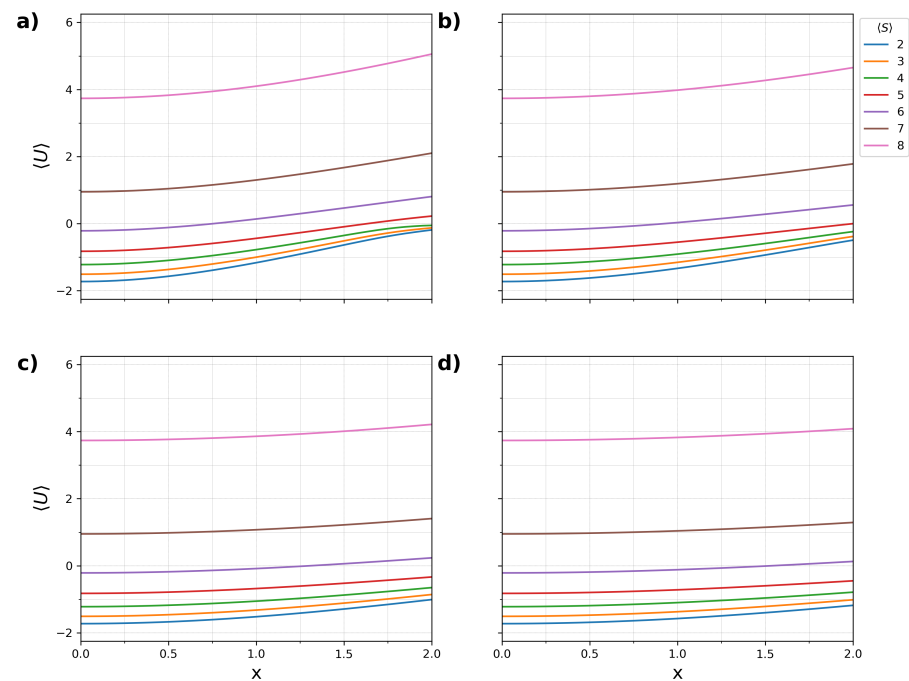


Figure 9. The behavior of the internal energy as a function of the dimensionless parameter x , at constant values of the entropy, is presented. The entropy S takes the values 2 to 8, in steps of one, in increasing order from the down curve to the up curve. As in the previous figures, (a–d) stand for values of the asymmetry parameter $\alpha = -1.25, -1.0, -0.75,$ and -0.362 , respectively.

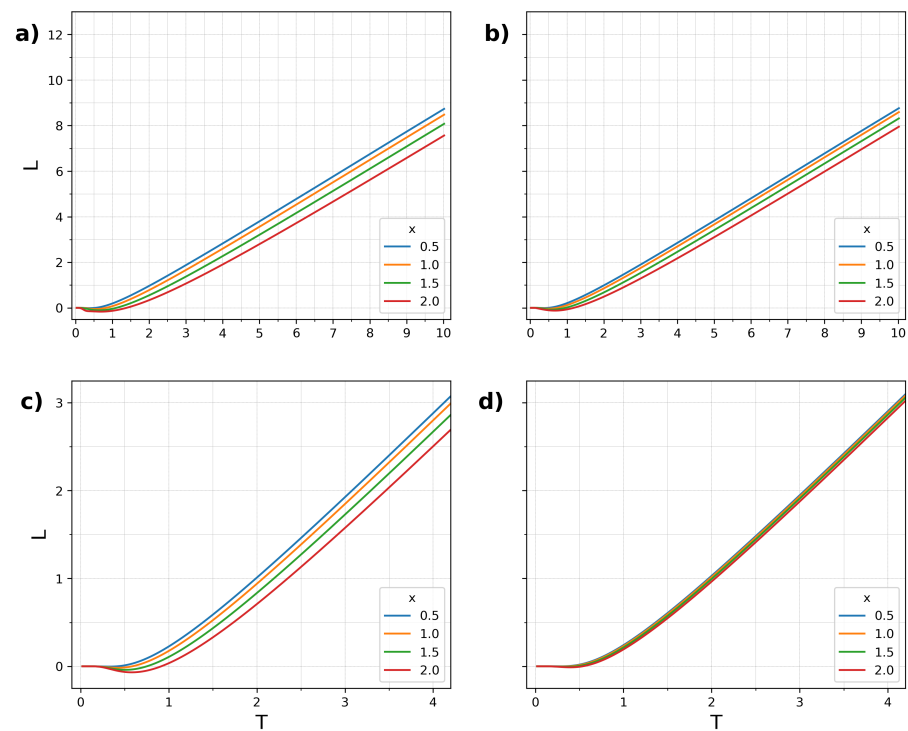


Figure 10. The mean value of $\hat{\mathcal{L}}$ as a function of the temperature are displayed. The curves correspond to different values of the dimensionless coupling constant x , from the up to the down curve x takes the values 0.5, 1, 1.5, and 2, respectively. (a–d) stand for values of the asymmetry parameter $\alpha = -1.25, -1.0, -0.75,$ and $-0.362,$ respectively.

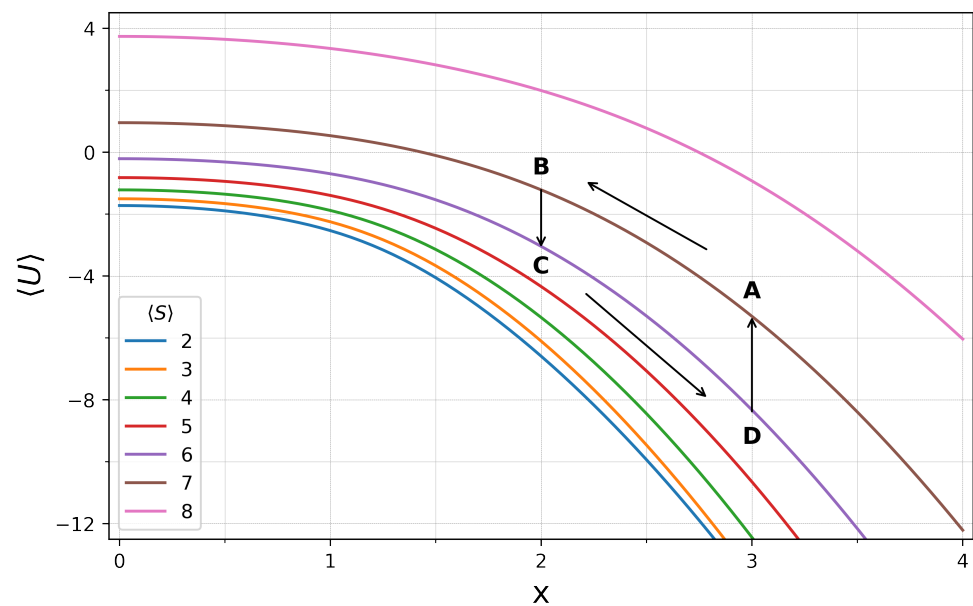


Figure 11. We displayed the general Otto cycle we have considered.

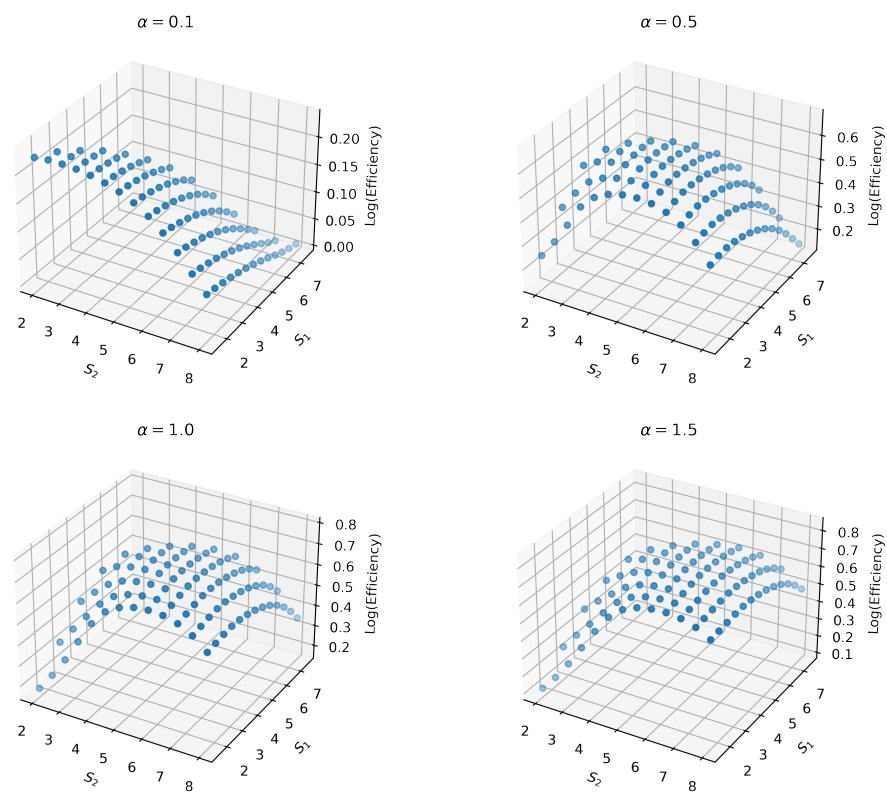


Figure 12. The maximum efficiency for the Otto cycle that works among two adiabatic curves, $s_1 < s_2$, is displayed in Figure for $\alpha = 0.1, 0.5, 1$, and 1.5 .

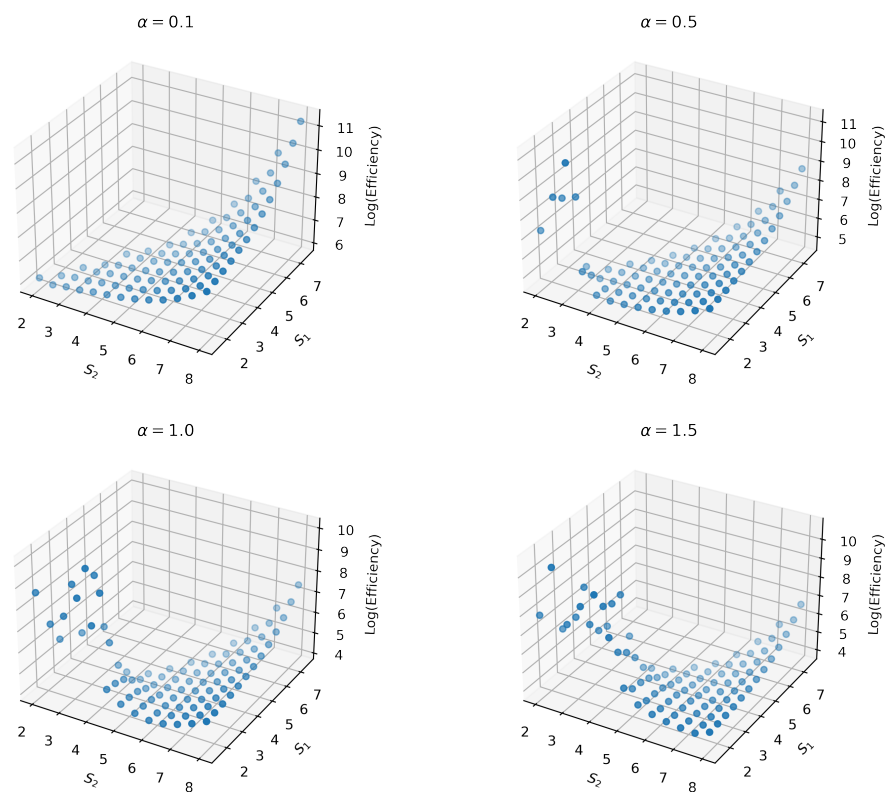


Figure 13. The maximum efficiency as a refrigerator of the Otto cycle that works among two adiabatic curves, $s_1 < s_2$, is displayed in the figure for the asymmetry parameter $\alpha = 0.1, 0.5, 1$, and 1.5 .

In Figures 8 and 9, we have displayed the behavior of the temperature and the internal energy, as a function of the dimensionless parameter x , at constant values of the entropy. The entropy S takes the values 2 to 8, in steps of one, in increasing order from the down curve to the up curve. As in the previous figures, panels (a), (b), (c), and (d), stand for values of the asymmetry parameter $\alpha = -1.25, -1.0, -0.75$, and -0.362 , respectively. The curves of the temperature and the internal energy show a softer variation with the coupling constants as compared with the corresponding results (Figures 4 and 5) for $\alpha > 0$.

The mean value of $\hat{\mathcal{L}}$ as a function of the temperature is depicted in Figure 10. The curves correspond to different values of the dimensionless coupling constant x . From the up to the down curve, x takes the values 0.5, 1, 1.5, and 2, respectively. Panels (a), (b), (c), and (d) stand for values of the asymmetry parameter $\alpha = -1.25, -1.0, -0.75$, and -0.362 , respectively. As can be observed from the figure, for the larger values of $|\alpha|$ at low temperatures, L takes negative values (condensate of spins). The mean value of $\hat{\mathcal{L}}$ increases with T .

From the previous results, it can be inferred that, in the computation of the partition function and of the thermodynamical properties derived from it, the effect of the presence of EPs is not significant. At a given α , the partition function is the trace of the density matrix over all the possible configurations of the system. For the present model, for large values of L , the EPs concentrate near values of α tending to zero. However, as seen from Figure 10, the mean values of $\hat{\mathcal{L}}$ are not larger than 10, even at high temperatures. The presence of the EPs should be relevant to other physical quantities, i.e., the survival probability in the study of the thermal evolution of an adequate initial state.

To complete the analysis of the system, we shall study the work that can be extracted from the hybrid system after an Otto cycle is performed. In Figure 11, we have drawn an Otto cycle. We performed work on the system from $A \rightarrow B$ along the adiabatic s_2 , heat is released from $B \rightarrow C$, the system performs work from $C \rightarrow D$ along the adiabatic s_1 , and heat is absorbed from $D \rightarrow A$ to return to the initial state. The coefficient of efficiency is defined as usual as the ratio of the absolute value of the net work conducted by the system to the heat absorbed (in our convention, the work conducted on the system is positive, and the one the system performs is negative, the same for the heat absorbed and the heat released), which is

$$e = \frac{Q_{BC} + Q_{DA}}{Q_{DA}}, \quad (11)$$

where we have taken into account the fact that the internal energy is conserved after performing a cycle, $\Delta U = Q_{BC} + Q_{DA} + W_{AB} + W_{DA} = 0$.

If the cycle is completed in the reverse direction, the system behaves as a refrigerator, with the efficiency given by

$$er = \frac{Q_{DA}}{Q_{BC} + Q_{DA}}. \quad (12)$$

In Figure 12, it is shown that the maximum value of the efficiency of the Otto cycle that works among two adiabatic curves, $s_1 < s_2$ for $\alpha = 0.1, 0.5, 1$, and 1.5 . The maximum values for the coefficient of efficiency are obtained by increasing the asymmetry parameter α .

The efficiency as a refrigerator of the inverse Otto cycle is presented in Figure 13, for values of $\alpha = 0.1, 0.5, 1.0$, and 1.5 , respectively. The maximum values for the coefficient of efficiency are obtained by decreasing the asymmetry parameter α .

The parameter α regulates the asymmetry between the pair creation and the pair destruction of a boson and a spin. For values of $\alpha > 1$, the interaction favors the destruction of pairs, and the system is efficient in working as a heat machine. On the other hand, for values of $\alpha < 1$, the interaction favors the production of pairs, and the system is efficient in working as a refrigerator.

For the sake of completeness, in Figure 14, we present results for the maximum efficiency of the Otto cycle that works among two adiabatic curves, $s_1 < s_2$, for negative asymmetry parameter $\alpha = -0.362$ and $\alpha = 1.25$.

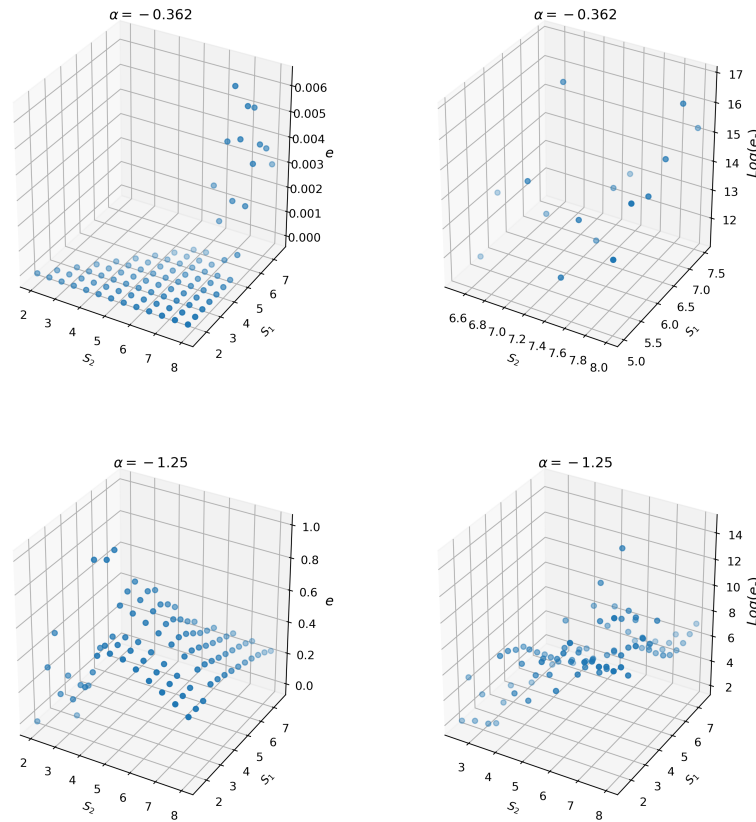


Figure 14. The maximum efficiency e , Equation (11) and er , of Equation (12), of the Otto cycle that works among two adiabatic curves, $s_1 < s_2$, is displayed in this figure for the asymmetry parameter $\alpha = -0.362$ and $\alpha = -1.25$.

As $\alpha \rightarrow 0$, the net work conducted on the system approaches zero, $|\Delta W| \rightarrow 0$, the same is true for the balance between the heat extracted and absorbed, $|\Delta Q| \rightarrow 0$. Thus, as $\alpha \rightarrow 0$, the efficiency as a heat machine is zero, but the efficiency as refrigerators becomes considerably large. This mechanism may serve as a way for cooling a hybrid system as the one of [39].

4. Conclusions

In this work, we have modified the model of Da Providencia and Schüte [31] by introducing an asymmetry factor in the interaction among the bosons and the spins. This asymmetry serves to take into account the imperfections of the environment, similar approaches have been used [32–34]. We have computed the exact partition function and from it the general thermodynamical properties of the hybrid system. The system undergoes a second-order phase transition as a function of the temperature, for different values of α . We have studied both the symmetry, $\alpha > 0$, and the broken symmetry dynamical phase, $\alpha < 0$.

We have presented results concerning the thermodynamical properties of the system in its broken symmetry phase. We observed that the presence of EPs does not have a significant effect on the partition function because, at a fixed α , all the possible configurations contribute to the trace of the temperature-dependent density matrix. Nevertheless, the presence of EPs may be relevant in analyzing other physical aspects of the problem, i.e., the temperature evolution of a particular initial state. At large values of the coupling constant and $|\alpha|$, though the partition function takes real values, anomalies in the thermodynamical

quantities can appear since we are working with an effective interaction which takes into account the effects of the environment, we are not working with the whole system [42–44].

For positive values of α , as the asymmetry parameter is increased, the critical temperature, for different values of the dimensionless coupling constant x , takes higher values. At constant entropy, both the internal energy and the temperature remain almost unchanged for values of $x \leq 1$. We performed an Otto cycle with this hybrid system as the working substance. The maximum values of the coefficient of efficiency are achieved by increasing α ; on the contrary, the maximum values for the efficiency of the system working as a refrigerator are obtained by decreasing the values of α . As pointed out before, the parameter α regulates the asymmetry between the pair creation and the pair destruction of a boson and a spin of the proposed interaction. For values of $\alpha > 1$, the interaction favors the destruction of pairs, and the system is efficient in working as a heat machine. On the other hand, for values of $\alpha < 1$, the interaction favors the production of pairs, and the system is efficient in working as a refrigerator. The introduction of an asymmetry factor, in the case $\alpha < 1$, allows for obtaining a very large efficiency of the system as a refrigerator. As $\alpha \rightarrow 0$, the net work completed on the system approaches zero, and the same is true for the balance between the heat extracted and absorbed. Thus, as $\alpha \rightarrow 0$, the efficiency as a heat machine is zero, but the efficiency as refrigerators becomes considerably large. This mechanism may serve as a way for cooling a hybrid system.

Work is in progress concerning the temperature-dependent evolution of a given initial state in the vicinity of EPs.

Author Contributions: Conceptualization, M.R. and D.T.; methodology, M.R. and D.T.; software, M.R. and D.T.; validation, M.R. and D.T.; formal analysis, M.R. and D.T.; investigation, M.R. and D.T.; resources, M.R. and D.T.; data curation, M.R. and D.T.; writing—original draft preparation, M.R. and D.T.; writing—review and editing, M.R. and D.T.; visualization, M.R. and D.T.; supervision, M.R. and D.T.; project administration, M.R. and D.T.; funding acquisition, M.R. and D.T. All authors have read and agreed to the published version of the manuscript.

Funding: This research was partially financial by CONICET, Argentine.

Data Availability Statement: Data is available upon reasonable request.

Acknowledgments: The authors are fellows of CONICET, Argentine.

Conflicts of Interest: The authors declare no conflict of interest.

References

1. Kurizki, G.; Kofman, A.G. *Thermodynamics and Control of Open Quantum Systems*; Cambridge University Press: Cambridge, UK, 2022.
2. Gemmer, J.; Michel, G.M.M. *Quantum Thermodynamics Emergence of Thermodynamic Behavior Within Composite Quantum Systems*; Springer: Berlin/Heidelberg, Germany, 2004.
3. von Lindenfels, D.; Gräß, O.; Schmiegelow, C.T.; Kaushal, V.; Schulz, J.; Mitchison, M.T.; Goold, J.; Schmidt-Kaler, F.; Poschinger, U.G. Spin Heat Engine Coupled to a Harmonic-Oscillator Flywheel. *Phys. Rev. Lett.* **2019**, *123*, 080602. [[CrossRef](#)] [[PubMed](#)]
4. Roßnagel, J.; Dawkins, S.T.; Tolazzi, K.N.; Abah, O.; Lutz, E.; Schmidt-Kaler, F.; Singer, K. A single-atom heat engine. *Science* **2016**, *352*, 325–329. [[CrossRef](#)] [[PubMed](#)]
5. Abah, O.; Roßnagel, J.; Jacob, G.; Deffner, S.; Schmidt-Kaler, F.; Singer, K.; Lutz, E. Single-Ion Heat Engine at Maximum Power. *Phys. Rev. Lett.* **2012**, *109*, 203006. [[CrossRef](#)] [[PubMed](#)]
6. Zanin, G.; Häffner, T.; Talarico, M.; Duzzioni, E.; Ribeiro, P.; Landi, G.T.; Céleri, L.C. Experimental quantum thermodynamics with linear optics. *Braz. J. Phys.* **2019**, *49*, 783–798. [[CrossRef](#)]
7. Jarzynski, C. Nonequilibrium Equality for Free Energy Differences. *Phys. Rev. Lett.* **1997**, *78*, 2690–2693. [[CrossRef](#)]
8. Deffner, S.; Jarzynski, C. Information Processing and the Second Law of Thermodynamics: An Inclusive, Hamiltonian Approach. *Phys. Rev. X* **2013**, *3*, 041003. [[CrossRef](#)]
9. Jarzynski, C.; Wójcik, D.K. Classical and Quantum Fluctuation Theorems for Heat Exchange. *Phys. Rev. Lett.* **2004**, *92*, 230602. [[CrossRef](#)]
10. Mandal, D.; Quan, H.T.; Jarzynski, C. Maxwell’s Refrigerator: An Exactly Solvable Model. *Phys. Rev. Lett.* **2013**, *111*, 030602. [[CrossRef](#)]
11. Strasberg, P.; Winter, A. First and Second Law of Quantum Thermodynamics: A Consistent Derivation Based on a Microscopic Definition of Entropy. *PRX Quantum* **2021**, *2*, 030202. [[CrossRef](#)]

12. Kosloff, R. Quantum Thermodynamics: A Dynamical Viewpoint. *Entropy* **2013**, *15*, 2100–2128. [[CrossRef](#)]
13. Dong, H.; Reiche, D.; Hsiang, J.T.; Hu, B.L. Quantum Thermodynamic Uncertainties in Nonequilibrium Systems from Robertson-Schrödinger Relations. *Entropy* **2022**, *24*, 870. [[CrossRef](#)] [[PubMed](#)]
14. Juan-Delgado, A.; Chenu, A. First law of quantum thermodynamics in a driven open two-level system. *Phys. Rev. A* **2021**, *104*, 022219. [[CrossRef](#)]
15. Millen, J.; Xuereb, A. Perspective on quantum thermodynamics. *New J. Phys.* **2016**, *18*, 011002. [[CrossRef](#)]
16. Hewgill, A.; Ferraro, A.; De Chiara, G. Quantum correlations and thermodynamic performances of two-qubit engines with local and common baths. *Phys. Rev. A* **2018**, *98*, 042102. [[CrossRef](#)]
17. de Lima Bernardo, B. Unraveling the role of coherence in the first law of quantum thermodynamics. *Phys. Rev. E* **2020**, *102*, 062152. [[CrossRef](#)]
18. Talkner, P.; Lutz, E.; Hänggi, P. Fluctuation theorems: Work is not an observable. *Phys. Rev. E* **2007**, *75*, 050102. [[CrossRef](#)]
19. Silva, T.A.B.P.; Angelo, R.M. Quantum mechanical work. *Phys. Rev. A* **2021**, *104*, 042215. [[CrossRef](#)]
20. Hong, Y.; Xiao, Y.; He, J.; Wang, J. Quantum Otto engine working with interacting spin systems: Finite power performance in stochastic thermodynamics. *Phys. Rev. E* **2020**, *102*, 022143. [[CrossRef](#)]
21. Del Grosso, N.F.; Lombardo, F.C.; Mazzitelli, F.D.; Villar, P.I. Quantum Otto cycle in a superconducting cavity in the nonadiabatic regime. *Phys. Rev. A* **2022**, *105*, 022202. [[CrossRef](#)]
22. Sindona, A.; Goold, J.; Gullo, N.L.; Plastina, F. Statistics of the work distribution for a quenched Fermi gas. *New J. Phys.* **2014**, *16*, 045013. [[CrossRef](#)]
23. Vicari, E. Particle-number scaling of the quantum work statistics and Loschmidt echo in Fermi gases with time-dependent traps. *Phys. Rev. A* **2019**, *99*, 043603. [[CrossRef](#)]
24. Bender, C.M.; Boettcher, S. Real Spectra in Non-Hermitian Hamiltonians Having *PT* Symmetry. *Phys. Rev. Lett.* **1998**, *80*, 5243–5246. [[CrossRef](#)]
25. Bender, C.M. Making sense of non-Hermitian Hamiltonians. *Rep. Prog. Phys.* **2007**, *70*, 947. [[CrossRef](#)]
26. Mostafazadeh, A. Pseudo-Hermiticity and generalized *PT*- and *CPT*-symmetries. *J. Math. Phys.* **2003**, *44*, 974–989. [[CrossRef](#)]
27. Znojil, M. Special Issue “Pseudo-Hermitian Hamiltonians in Quantum Physics in 2014”. *Int. J. Theor. Phys.* **2015**, *54*, 3867–3870. [[CrossRef](#)]
28. Deffner, S.; Saxena, A. Jarzynski Equality in *PT*-Symmetric Quantum Mechanics. *Phys. Rev. Lett.* **2015**, *114*, 150601. [[CrossRef](#)]
29. Gardas, B.; Deffner, S.; Saxena, A. Non-Hermitian quantum thermodynamics. *Sci. Rep.* **2016**, *6*, 23408. [[CrossRef](#)]
30. Santos, J.F.G.; Luiz, F.S. Quantum thermodynamics aspects with a thermal reservoir based on \mathcal{P} -symmetric Hamiltonians. *J. Phys. Math. Theor.* **2021**, *54*, 335301. [[CrossRef](#)]
31. Schütte D.; Providencia, J.D. A solvable model of boson condensation. *Nucl. Phys. A* **1977**, *282*, 518–532. [[CrossRef](#)]
32. Clements, W.R.; Renema, J.J.; Eckstein, A.; Valido, A.A.; Lita, A.; Gerrits, T.; Nam, S.W.; Kolthammer, W.S.; Huh, J.; Walmsley, I.A. Approximating vibronic spectroscopy with imperfect quantum optics. *J. Phys. B At. Mol. Opt. Phys.* **2018**, *51*, 245503. [[CrossRef](#)]
33. Ma, S.L.; Li, P.B.; Fang, A.P.; Gao, S.Y.; Li, F.L. Dissipation-assisted generation of steady-state single-mode squeezing of collective excitations in a solid-state spin ensemble. *Phys. Rev. A* **2013**, *88*, 013837. [[CrossRef](#)]
34. Ramírez R., Reboiro M., T.D. Exceptional Points from the Hamiltonian of a hybrid physical system: Squeezing and anti-Squeezing. *Eur. Phys. J. D* **2020**, *74*, 193. [[CrossRef](#)]
35. Baumann, K.; Guerlin, C.; Brennecke, F.; Esslinger, T. Dicke quantum phase transition with a superfluid gas in an optical cavity. *Nature* **2010**, *464*, 1301–1306. [[CrossRef](#)] [[PubMed](#)]
36. Sachdev, S. Quantum phase transitions. *Phys. World* **1999**, *12*, 33. [[CrossRef](#)]
37. Meyer-ter Vehn, J. Unnatural parity states in nuclei and pion condensation. *Phys. Rep.* **1981**, *74*, 323–378. [[CrossRef](#)]
38. Nazarewicz, W. Microscopic origin of nuclear deformations. *Nucl. Phys. A* **1994**, *574*, 27–49. [[CrossRef](#)]
39. Feist, A.; Huang, G.; Arend, G.; Yang, Y.; Henke, J.W.; Raja, A.S.; Kappert, F.J.; Wang, R.N.; Lourenço-Martins, H.; Qiu, Z.; et al. Cavity-mediated electron-photon pairs. *Science* **2022**, *377*, 777–780. [[CrossRef](#)]
40. Civitarese, O.; Reboiro, M. Exactly solvable fermion-boson mapping representations. *Phys. Rev. C* **1998**, *57*, 3055. [[CrossRef](#)]
41. Civitarese, O.; Reboiro, M. Boson mapping at finite temperature: An application to the thermo field dynamics. *Phys. Rev. C* **1999**, *60*, 034302. [[CrossRef](#)]
42. Thirring, W. Systems with negative specific heat. *Z. Phys. Hadron. Nucl.* **1970**, *235*, 339. [[CrossRef](#)]
43. Ingold, G.L.; Hänggi, P.; Talkner, P. Specific heat anomalies of open quantum systems. *Phys. Rev. E* **2009**, *79*, 061105. [[CrossRef](#)] [[PubMed](#)]
44. Strzys, M.P.; Anglin, J.R. Negative specific heat with trapped ultracold quantum gases. *New J. Phys.* **2014**, *16*, 013013. [[CrossRef](#)]